Received: 15 May 2022 | Revised: 8 July 2022 | Accepted: 1 August 2022

DOI: 10.1111/omi.12384

ORIGINAL ARTICLE

WILEY

Fluorescence lectin binding analysis of carbohydrate components in dental biofilms grown in situ in the presence or absence of sucrose

Irene Dige[1] | Pune N. Paqué[2,3] | Yumi Chokyu Del Rey[1] | Marie Braad Lund[4] | Andreas Schramm[4] | Sebastian Schlafer[1]

[1]Section for Oral Ecology and Caries Control, Department of Dentistry and Oral Health, Aarhus University, Aarhus, Denmark

[2]Clinic of Reconstructive Dentistry, Center of Dental Medicine, University of Zurich, Zurich, Switzerland

[3]Division of Oral Microbiology and Immunology, Clinic of Conservative and Preventive Dentistry, Center of Dental Medicine, University of Zurich, Zurich, Switzerland

[4]Section for Microbiology, Department of Biology, Aarhus University, Aarhus, Denmark

Correspondence
Sebastian Schlafer and Irene Dige, Section for Oral Ecology and Caries Control, Department of Dentistry and Oral Health, Aarhus University, Vennelyst Boulevard 9, 8000 Aarhus C, Denmark.
Email: sebastians@dent.au.dk; idige@dent.au.dk

Funding information
Danish Dental Association (FORSKU)

Abstract

Carbohydrate components, such as glycoconjugates and polysaccharides, are constituents of the dental biofilm matrix that play an important role in biofilm stability and virulence. Exopolysaccharides in *Streptococcus mutans* biofilms have been characterized extensively, but comparably little is known about the matrix carbohydrates in complex, in situ-grown dental biofilms. The present study employed fluorescence lectin binding analysis (FLBA) to investigate the abundance and spatial distribution of glycoconjugates/polysaccharides in biofilms ($n = 306$) from 10 participants, grown in situ with (SUC) and without (H2O) exposure to sucrose. Biofilms were stained with 10 fluorescently labeled lectins with different carbohydrate specificities (AAL, ABA, ASA, HPA, LEA, MNA-G, MPA, PSA, VGA and WGA) and analyzed by confocal microscopy and digital image analysis. Microbial composition was determined by 16S rRNA gene sequencing. With the exception of ABA, all lectins targeted considerable matrix biovolumes, ranging from 19.3% to 194.0% of the microbial biovolume in the biofilms, which illustrates a remarkable variety of carbohydrate compounds in in situ-grown dental biofilms. MNA-G, AAL, and ASA, specific for galactose, fucose, and mannose, respectively, stained the largest biovolumes. AAL and ASA biovolumes were increased in SUC biofilms, but the difference was not significant due to considerable biological variation. SUC biofilms were enriched in streptococci and showed reduced abundances of *Neisseria* and *Haemophilus* spp., but no significant correlations between lectin-stained biovolumes and bacterial abundance were observed. In conclusion, FLBA demonstrates the presence of a voluminous biofilm matrix comprising a variety of different carbohydrate components in complex, in situ-grown dental biofilms.

KEYWORDS
16S rRNA sequencing, biofilm, confocal laser scanning microscopy, extracellular polymeric substances, fluorescence lectin binding analysis, glycoconjugates, in situ

1 | INTRODUCTION

Carbohydrates are important constituents of the dental biofilm matrix (Bowen et al., 2018; Karygianni et al., 2020). Glycoconjugates and extracellular polysaccharides contribute to cellular adhesion, cell-to-cell interactions, biofilm stability, and nutrition (Jakubovics et al., 2021). Mutans and dextrans, which are the predominant extracellular polysaccharides in laboratory biofilms of *Streptococcus mutans*, have been characterized extensively (Banas & Vickerman, 2003; Cugini et al., 2019; Falsetta et al., 2014), but there are comparably little data on the occurrence and spatial distribution of glycoconjugates and polysaccharides in the matrix of complex, in situ-grown dental biofilms.

Fluorescently labeled fungal or plant-derived lectins with high affinities to different carbohydrate moieties can be used to target and visualize glycoconjugate components or polysaccharides inside the dental biofilm matrix. Some studies have employed Concanavalin A (ConA) or wheat germ agglutinin (WGA), both of which are widely used in other biological applications, to visualize glucans in dental biofilms (Gonçalves et al., 2015; Hannig et al., 2013; Hertel, Pötschke, et al., 2017; Hertel, Wolf, et al., 2017; Lester & Simmonds, 2012). A recent study followed a comprehensive approach and investigated the binding properties of 75 different fluorescently labeled lectins in pooled dental plaque and in biofilms grown in situ in the absence of sucrose (Tawakoli et al., 2017). Tawakoli et al. identified 10–12 different lectins that proved particularly suitable to target glycoconjugates in the dental biofilm matrix.

The aim of the present work was to study the binding properties of the shortlisted lectins in dental biofilms grown in situ for 48 h in the presence and absence of sucrose. Lectin binding patterns and relative biovolumes of the targeted matrix components were analyzed quantitatively by confocal laser scanning microscopy (CLSM) and subsequent digital image analysis (DIA), and correlated to the microbial composition of the biofilms, as determined by next generation sequencing.

2 | MATERIALS AND METHODS

2.1 | Collection of in situ-grown biofilms

Ten healthy participants (22–26 years; average 23.7 years, all females) were recruited for the study. Subjects suffering from chronic systemic disease and subjects who had received antibiotic therapy within the past 6 months were excluded, as well as pregnant and breastfeeding women. The participants showed no signs of active carious lesions or periodontal disease. The experimental protocol was approved by the Ethics Committee of Region Midt, Denmark (ID: 1-10-72-162-17), and the project was registered in the internal database of research projects at Aarhus University. Written informed consent was obtained from all participants.

Based on alginate impressions, individually designed lower jaw splints were manufactured for all participants. The splints harboured glass carriers with a surface roughness corresponding to natural enamel (1200 grit; 4 × 4 × 1.5 mm; Menzel, Braunschweig, Germany) for biofilm collection. The participants wore the splints for periods of 48 h, during which one side of the splint was exposed to sucrose (4%; 8 × 2 min per day) and the other side to physiological saline. The splints were only removed for sucrose/water treatment, during the intake of foods or drinks other than water and during oral hygiene procedures.

For each investigated lectin and treatment type (sucrose/water), triplicate biofilms were collected, resulting in a total of 306 biofilms. Additionally, one biofilm from each participant and treatment type ($n = 20$) was collected for 16S rRNA gene sequencing. After growth, the glass slabs were removed from the splints and the biofilms were fixed in paraformaldehyde (3.5% in phosphate-buffered saline [PBS]; 3 h; 4°C). Thereafter, glass slabs were washed three times with PBS and stored in PBS/ethanol (1:1 [v/v]) at −20°C until experimental use.

2.2 | Fluorescence lectin binding analysis

Three participants were randomly selected to investigate the binding of all lectins employed in the present study: *Aleuria aurantia* lectin (AAL), *Agaricus bisporus* agglutinin (ABA), *Allium sativum* agglutinin (ASA), *Helix pomatia* agglutinin (HPA), *Lycopersicon esculentum* agglutinin (LEA), *Morniga* agglutinin *G* (MNA-G), *Maclura pomifera* agglutinin (MPA), *Pisum sativum* agglutinin (PSA), *Vicia graminea* agglutinin (VGA), and Wheat germ agglutinin (WGA). All lectins were fluorescently labeled with fluorescein isothiocyanate (FITC) and used at a working concentration of 100 μM. The origin, carbohydrate specificity, and suppliers of the lectins are listed in Tables 1 and S1.

Fluorescence lectin binding analysis (FLBA) was performed as described previously (Neu & Lawrence, 1999). Briefly, the biofilms were incubated with the respective FITC-labeled lectins for 30 min at room temperature, washed three times with PBS, and then counterstained with SYTO 60 (10 μM; 15 min; Molecular probes, Thermo Fisher, Carlsbad, USA) to visualize microorganisms. The glass slabs were placed in 96-well plates for microscopy (Ibidi GmbH, Gräfelfing, Germany), with the biofilms facing downward, and imaged with a CLSM. Based on the results obtained from three participants, the lectins AAL, ASA, and MNA-G were selected for further analysis and were used to visualize carbohydrate structures in biofilms collected from the remaining seven participants ($n = 126$).

2.3 | CLSM and image analysis

Biofilms were analysed with an inverted confocal microscope (Zeiss LSM 700, Jena, Germany) equipped with a 63× objective (alpha Plan-Apochromat, Zeiss). FITC-labeled lectins were excited at 488 nm, SYTO 60 was excited at 639 nm. Detection was performed with the beam splitter set to 640 nm. In each of the biofilm specimens, 3-sliced *z*-stacks spanning the height of the biofilms were acquired in six

TABLE 1 Employed fluorescently labeled lectins

Lectin	Abbreviation	Origin	Carbohydrate specificity	Fluorescence signal
Aleuria aurantia lectin	AAL	Orange peel fungus	Fucose (α1–6) *N*-Acetylglucosamine, Fucose (α1–3) *N*-Acetyllactosamine	Strong
Agaricus bisporus agglutinin	ABA	Button mushroom	Galactose (β1–3) *N*-Acetylgalactosamine	Low
Allium sativum agglutinin	ASA	Garlic	Mannose	Strong
Helix pomatia agglutinin	HPA	Burgundy snail	*N*-Acetylgalactosamine	Intermediate
Lycopersicon esculentum agglutinin	LEA	Tomato	(β1–4) *N*-Acetylglucosamine	Strong
Morniga agglutinin G	MNA-G	Black mulberry	Galactose >> Mannose/Glucose	Strong
Maclura pomifera agglutinin	MPA	Osage orange	*N*-Acetylgalactosamine > Galactose	Intermediate
Pisum sativum agglutinin	PSA	Pea	α-Mannose > α-Glucose	Intermediate
Vicia graminea agglutinin	VGA	Vetch	O-linked D-galactose (β1–3) *N*-Acetylgalactosamine	Intermediate
Wheat germ agglutinin	WGA	Wheat	(*N*-Acetylglucosamine)2, *N*-Acetylneuraminic acid	Intermediate

predefined equidistant positions. The images were 1192 × 1192 pixels in size (101.6 × 101.6 μm) and captured with a pixel dwell time of 1.1 μs and the pinhole set to 1 AU (0.9 μm optical slice). Laser power (488 nm) and detector gain were kept constant for each fluorescently labeled lectin.

CLSM images were subjected to qualitative visual assessment and to DIA. Visual assessment was performed by two independent observers. The strength of the lectins' fluorescence signals was rated (strong, intermediate, weak) and typical lectin binding patterns were identified. For DIA, images were exported to the software daime (Daims et al., 2006), and the areas covered by microorganisms and carbohydrate structures were determined in each image by segmentation based on brightness thresholds. Microbial and carbohydrate biovolumes were estimated in each *z*-stack according to the Cavalieri principle, by multiplying the interslice distance with the total area in all three images of a stack (Gundersen & Jensen, 1987). Carbohydrate biovolumes were then normalized to the microbial biovolumes in each *z*-stack.

Lectin-targeted carbohydrates in the biofilms were either found in direct association with microbial cells (presumably attached to the cell wall) or in cell-free areas of the biofilms. To specifically quantify those carbohydrate structures that were not attached to microbial cell surfaces (intercellular glycoconjugates/polysaccharides), lectin-stained biovolumes that did not overlap with microbial cells were quantified separately in all images. To do so, the object masks of the areas covered by glycoconjugates/polysaccharides and microorganisms were extracted, and the lectin-stained areas without overlapping microorganisms were determined in each image. For each *z*-stack, intercellular glycoconjugate/polysaccharide biovolumes were estimated according to the Cavalieri principle. The DIA procedure is illustrated in Figure S1.

Wilcoxon signed rank tests were used to assess differences in biofilm height, microbial biovolume, and lectin-stained biovolumes (total and intercellular) between biofilms grown in the presence and absence of sucrose. Statistical analyses were performed in R v. 4.1.2 (R Core Team, 2021).

2.4 | rRNA gene sequencing

DNA extraction from the glass slabs, polymerase chain reaction (PCR), and sequencing of the bacterial 16S rRNA gene amplicons were performed as described in detail previously (Tawakoli et al., 2017). In brief, enzymatic lysis was combined with the PowerLyzer PowerSoil DNA Isolation Kit (Qiagen Denmark) for efficient DNA extraction; the V3–V4 region of bacterial 16S rRNA genes was amplified using primers Bac 341F and Bac 805R (Herlemann et al., 2011) and paired-end sequenced (2 × 300 bp) on an Illumina MiSeq sequencer.

2.5 | rRNA gene sequence analysis

All analyses were done in R v. 4.1.2 (R Core Team, 2021). Sequences were trimmed to remove barcodes and primers using cutadapt v. 0.1.1 (Martin, 2011). "DADA2" v. 1.18.0 (Callahan et al., 2016) was used for identifying amplicon sequence variants (ASVs) and taxonomic classification according to Silva SSU reference database no. 138 (Quast et al., 2013). After taxonomic classification, the ASVs were filtered to only include those classified as Bacteria. Nucleic acid extraction blanks and PCR negatives were used for decontaminating the data using the R package Decontam v. 1.10.0 (Davis et al., 2018). Putative contaminants were identified using the prevalence method with a threshold of 0.1 and were subsequently removed from the data. All further data analysis was done using the R packages Phyloseq v. 1.34.0 (McMurdie & Holmes, 2013), Microbiome v. 1.12.0 (Lahti et al., 2017), vegan v. 2.5.7 (Oksanen et al., 2019), ggplot2 v. 3.3.5 (Wickham, 2016), and custom R scripts.

Alpha diversity (as observed ASV richness and Shannon index) was calculated on a normalized dataset subsampled to 7238 reads per sample. A principal component analysis was carried out on read counts normalized by centered log-ratio (clr) transformation (as implemented in the microbiome R package). Differentially abundant genera in paired

samples between the two treatments (sucrose and water) were identified using the Wilcoxon signed-rank test on clr transformed read counts. The *p*-values were adjusted for false discovery rate using the Benjamini–Hochberg method and 0.05 was used as the significance cutoff for the adjusted *p*-values (*q*-values).

Sequence data have been deposited to GenBank under BioProject PRJNA833942. ASV sequences, taxonomic classification, read counts, and relevant metadata can be found in Tables S2 and S3.

3 | RESULTS

3.1 | Biofilm growth

Biofilm growth on the glass carriers was robust, with average thickness (± SD) for the different subjects ranging from 9.5 μm (2.9) to 21.2 μm (7.2). All biofilms (biofilms grown in the presence and in the absence of sucrose) comprised cells of various morphology and showed typical features of dental biofilms. Thin, sheet-like areas alternated with dense, mushroom-shaped protuberations, and both densely colonized and large cell-free areas were observed. Biofilms grown in the presence of sucrose were thicker than biofilms grown in the absence of sucrose (18.5 μm ± 4.8 SD vs. 15.5 μm ± 4.1 SD; $p < 0.05$), but the microbial biovolumes did not differ between both types of biofilms ($p = 0.64$), indicating that biofilms in the sucrose group displayed larger matrix biovolumes. In some instances, biofilm samples could not be evaluated quantitatively due to the deposition of human epithelial cells on the glass carriers or insufficient biofilm growth.

3.2 | FLBA of the lectins AAL, ABA, ASA, HPA, LEA, MNA-G, MPA, PSA, VGA, and WGA in biofilms from three subjects

The binding properties of all 10 employed lectins were investigated in biofilms ($n = 180$) from three study participants.

3.3 | Qualitative analysis of lectin binding

Fluorescence intensities and binding patterns of all lectins were assessed visually by two independent observers. AAL, ASA, LEA, and MNA-G showed the strongest fluorescence signals (Table 1), and the binding patterns varied considerably between different lectins. Some lectins mainly targeted the surface layer of the biofilms (LEA), while other lectins bound glycoconjugates/polysaccharides located inside of dense bacterial clusters (PSA, ASA, AAL). Some lectins (MPA, VGA) predominantly attached to microbial cell surfaces, while other lectins (MNA-G, AAL) bound strongly to cell-free areas inside the biofilms. Representative images of lectin binding patterns and intensities are shown in Figure S2.

3.4 | Quantitative analysis of lectin binding

The biovolumes visualized by fluorescently labeled lectins were normalized against the microbial biovolumes in all examined biofilms (Figure 1a). In biofilms grown in the absence of sucrose, MNA-G stained the largest biovolume (194.0% ± 107.9 SD of the microbial biovolume), followed by WGA (108.8% ± 49.8 SD), AAL (89.4% ± 36.9 SD), and ASA (72.4% ± 44.8 SD). In biofilms exposed to sucrose during growth, AAL targeted the largest biovolume (173.4% ± 219.1 SD), followed by ASA (162.8% ± 143.8 SD), MNA-G (148.8% ± 129.9 SD), and WGA (105.9% ± 61.5 SD). The lectins ABA, HPA, MPA, and VGA stained only minor parts of the biofilm matrix (<50% of the microbial biovolume). MNA-G, WGA, PSA, and HPA visualized similar biovolumes in biofilms grown with and without the presence of sucrose. Hence, they may bind to fundamental matrix components that are not induced by sucrose exposure. In contrast, AAL and ASA targeted larger matrix biovolumes in biofilms grown in the presence of sucrose, whereas the opposite was true for LEA, MPA, and VGA. Representative images of the lectins that visualized the largest biovolumes are shown in Figure 1b.

In addition to the total biovolume targeted by the different lectins, we also quantified the biovolumes of glycoconjugates or polysaccharides that were not directly associated to microbial cell walls (see Figure S1). These intercellular biovolumes differed markedly, ranging from 38.1% (LEA) to 72.3% (AAL) of the total biovolume targeted by the respective lectin (Figure 2). Across all biofilms from three participants, AAL, MNA-G, and ASA visualized the largest total biovolumes and the largest intercellular biovolumes. Therefore, these three lectins were selected for subsequent experiments involving the remaining seven participants.

3.5 | FLBA of the lectins AAL, ASA, and MNA-G in biofilms from 10 subjects

The binding of AAL, ASA, and MNA-G was investigated in biofilms ($n = 126$) from additional seven study participants. Across all 10 subjects, ASA, MNA-G, and AAL visualized 118.4% (± 46.7 SD), 100.6% (± 95.0 SD), and 97.0% (± 37.8 SD), respectively, of the microbial biovolume in biofilms grown in the absence of sucrose. As observed for the first three participants, biovolumes stained by MNA-G were similar for biofilms grown in the presence of sucrose (100.3% ± 104.3 SD). ASA (143.2% ± 105.1 SD) and especially AAL (170.5% ± 178.5 SD) visualized larger areas in biofilms that were exposed to sucrose (Figure 3a). Due to considerable interindividual variation (Figure S3), these differences were not statistically significant.

About half (54.3%) of the glycoconjugate/polysaccharide biovolume visualized by MNA-G was not associated to bacterial cell surfaces (intercellular carbohydrate structures), with no difference between biofilms grown in the presence and absence of sucrose (54.8% vs. 53.8%). A total of 52.6% and 64.6% of the biovolumes visualized by ASA and AAL were intercellular carbohydrate structures. For both lectins, the binding to intercellular carbohydrate structures was increased in

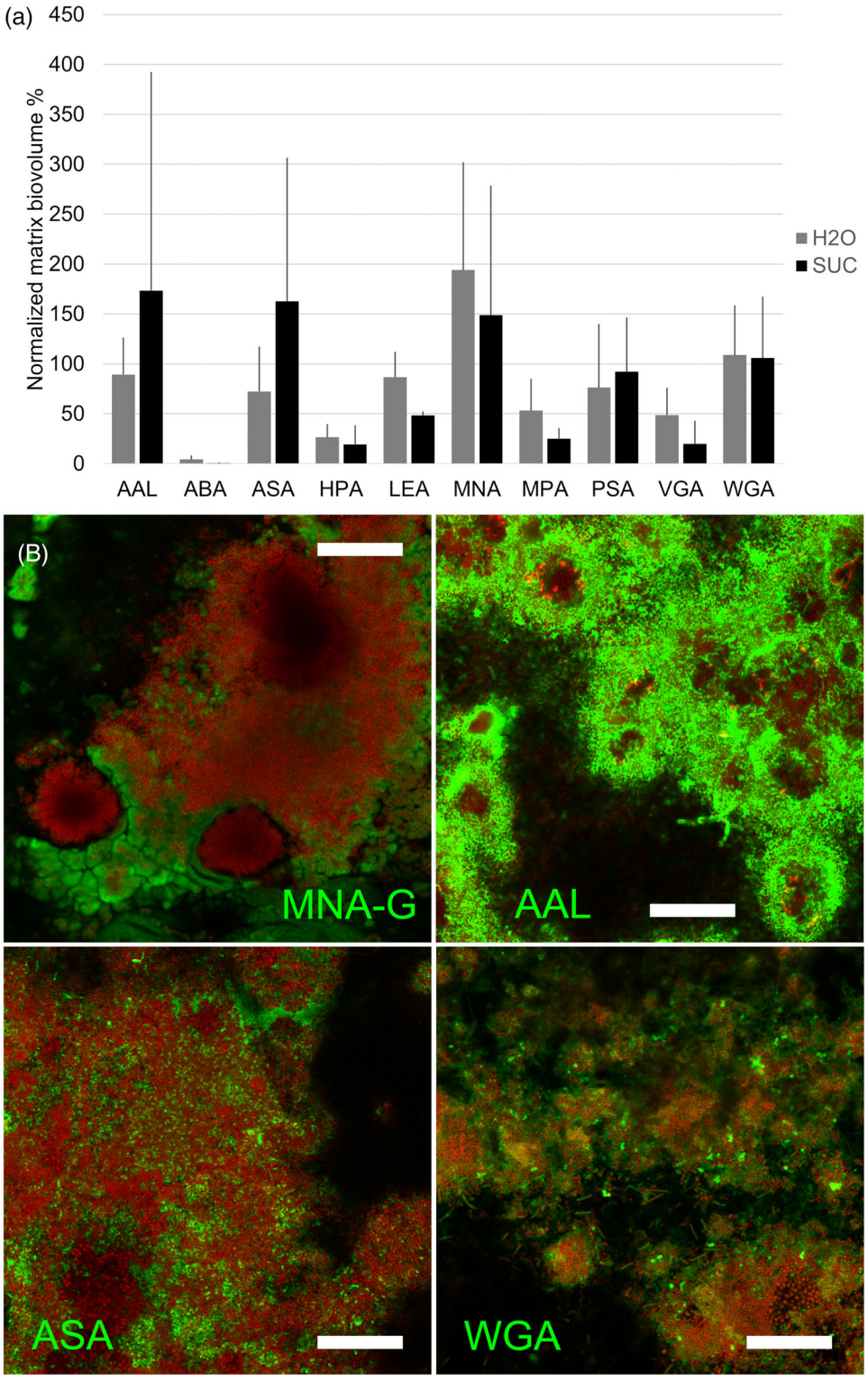

FIGURE 1 Carbohydrate biovolumes visualized by 10 different lectins in biofilms from three participants. (a) A total of 180 biofilms were stained using the fluorescently labeled lectins AAL, ABA, ASA, HPA, LEA, MNA-G, MPA, PSA, VGA, and WGA. MNA-G, AAL, ASA, and WGA visualized the largest glycoconjugate/polysaccharide biovolumes in the examined biofilms. MNA-G, WGA, PSA, and HPA targeted similar biovolumes in biofilms grown in the presence (SUC) and absence (H2O) of sucrose. AAL and ASA visualized larger biovolumes in biofilms grown in the presence of sucrose, while the opposite was observed for LEA, MPA, and VGA. Error bars = SD. (b) Representative images of glycoconjugates/polysaccharides visualized by the fluorescently labeled lectins MNA-G, AAL, ASA, and WGA (green). Microbial cells were stained with SYTO 60 (red). Bars = 20 μm

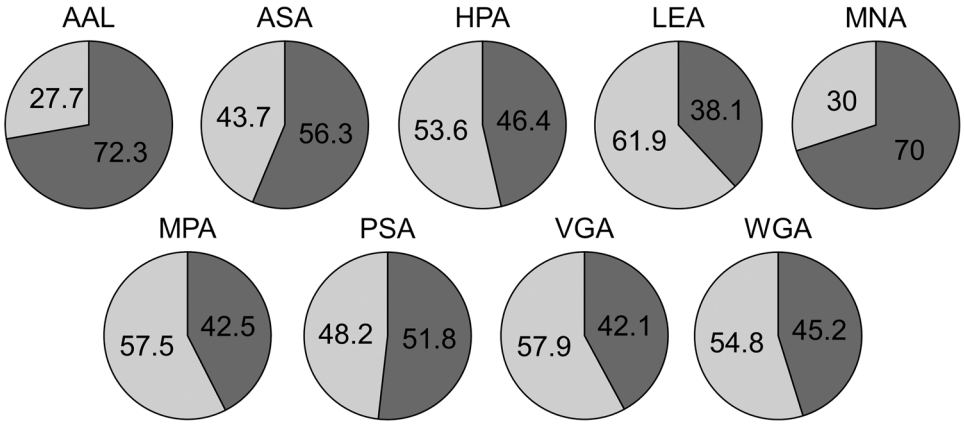

FIGURE 2 Percentage of lectin-stained carbohydrate biovolumes on microbial cell surfaces and in cell-free areas of biofilms from three participants. Some of the lectin-stained glycoconjugates/polysaccharides were associated to microbial cell surfaces (light gray), while others were located in cell-free areas of the biofilms (intercellular glycoconjugates/polysaccharides; dark gray). The percentage of intercellular carbohydrate components visualized by the lectins AAL, ABA, ASA, HPA, LEA, MNA-G, MPA, PSA, VGA, and WGA ranged from 38.1% (LEA) to 72.3% (AAL).

biofilms that were grown in the presence of sucrose (ASA 59.2% vs. 44.7%; AAL 76.7% vs. 43.3%) (Figure 3b). Figure 3c illustrates typical binding patterns for AAL and ASA in both types of biofilms.

3.6 | Biofilm bacterial community composition

Between 39 and 367 ASVs were observed per biofilm sample, and the Shannon index ranged from 1.28 to 4.12 (Table S2). The biofilms of all participants were strongly dominated by *Streptococcus* spp. (mean relative abundance of 0.61), with minor contributions of *Haemophilus* spp., *Veillonella* spp., *Fusobacterium* spp., *Granulicatella* spp., and *Neisseria* spp. (mean relative abundances ranging from 0.18 to 0.02). Other bacterial genera had mean relative abundances below 0.01 (Figure 4a; Table S3). Variation in the overall biofilm composition between participants was much larger than the changes induced by sucrose (Figure 4b), and neither richness nor diversity of the biofilm community differed significantly between the two treatments ($p = 0.63$ and $p = 0.50$, respectively). Likewise, PERMANOVA analysis showed no significant difference in the overall community composition between the two treatments ($p = 0.759$). Nevertheless, the relative abundance of *Streptococcus* spp. increased significantly in all sucrose-treated biofilms, while that of *Haemophilus* spp. and *Neisseria* spp. decreased (Figure 4c). In total, the relative abundance of 41 out of 226 genera was significantly different in the sucrose-treated biofilms (Table S4).

Spearman rank correlation tests showed no correlation between lectin biovolumes (AAL, ASA, and MNA-G) and the three most abundant and significantly differentially abundant genera (*Streptococcus*, *Haemophilus*, and *Neisseria*) (Table 2). In contrast, there was a significant negative correlation (Spearman; $R = -0.54$; $p = 0.026$) between MNA-G-bound biovolumes and the alpha diversity of the biofilm community (expressed as Shannon index), indicating that biofilms with higher microbial diversity had less galactose-containing carbohydrates in their matrix. No correlations were found between the biovolumes of AAL or ASA and microbial diversity (Figure S4).

TABLE 2 Spearman rank correlations between lectin biovolumes and the three most abundant genera with differential abundance in biofilms grown in the presence and absence of sucrose

Genus	Lectin	Rho	*p*-value
Streptococcus	AAL	−0.0959752	0.7048
Streptococcus	ASA	−0.1971104	0.4315
Streptococcus	MNA-G	0.4166667	0.0975
Neisseria	AAL	0.1517028	0.5467
Neisseria	ASA	−0.2033024	0.4168
Neisseria	MNA-G	−0.0294118	0.9134
Haemophilus	AAL	0.1826625	0.4666
Haemophilus	ASA	0.4385965	0.0702
Haemophilus	MNA-G	−0.2107843	0.4152

4 | DISCUSSION

The present study is the first to study the effect of sucrose exposure on the abundance and spatial distribution of carbohydrate components in in situ-grown dental biofilms by means of FLBA. The 10 investigated lectins (AAL, ABA, ASA, HPA, LEA, MNA-G, MPA, PSA, VGA, and WGA) had previously shown significant binding to glycoconjugates in a pooled plaque sample from different subjects (Tawakoli et al., 2017). All lectins penetrated well through the relatively thin biofilms, and with the exception of ABA, all lectins visualized considerable matrix biovolumes, ranging from 19.3% to 194.0% of the microbial biovolume of the biofilms.

Part of the lectin-stained biovolume was closely associated to microbial cells and likely represented cell wall constituents, such as oligo- or polysaccharide cell receptors or glycoproteins (Nobbs et al., 2009; Whittaker et al., 1996). The remaining targeted carbohydrate components were located between microbial clusters and had no direct contact to bacterial cells. These intercellular glycoconjugates/polysaccharides made up between 38.1% (LEA) and 72.3%

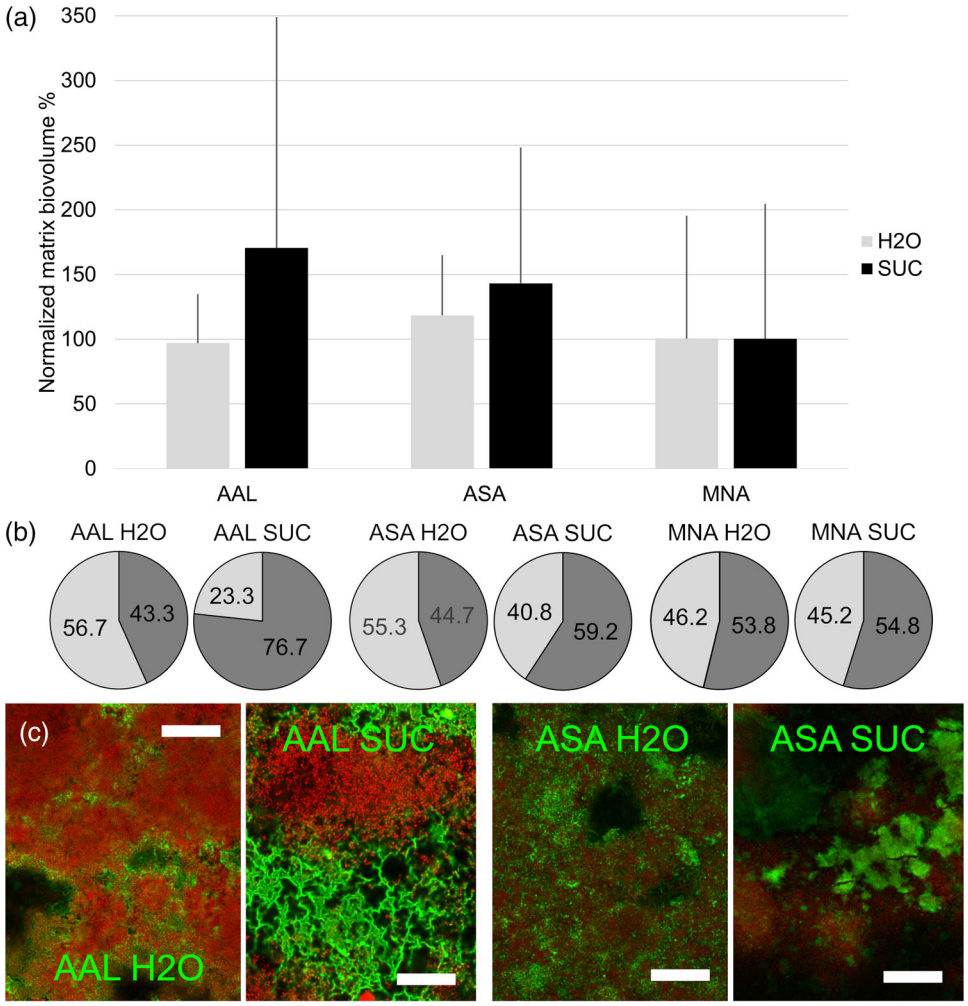

FIGURE 3 Carbohydrate components visualized by lectins AAL, ASA, and MNA-G in biofilms from 10 participants. (a) All three lectins showed extensive binding to matrix glycoconjugates/polysaccharides in the biofilms. Lectins ASA and especially AAL targeted larger areas in biofilms grown in the presence (SUC) than in the absence (H2O) of sucrose, albeit with considerable interindividual variation. (b) Some lectin-stained carbohydrate structures were associated with microbial cell surfaces (light gray), while others were located in cell-free areas of the biofilms (intercellular glycoconjugates/polysaccharides; dark gray). The percentage of intercellular glycoconjugates/polysaccharides targeted by ASA and especially AAL was higher in biofilms grown in the presence of sucrose. The binding pattern of MNA-G was not affected by exposure to sucrose during biofilm growth. (c) Representative images illustrate typical binding patterns of the FITC-labeled lectins AAL and ASA (green). Microbial cells were stained with SYTO 60 (red). Bars = 20 μm

(AAL, data for three participants) of the total lectin-stained biovolumes. The employed lectins covered a wide array of different carbohydrate specificities (see Table 1), which suggests a compositional diversity of the glycoconjugate/polysaccharide matrix of in situ-grown biofilms that has received little attention. Notably, none of the lectins used in the present study had a high affinity to glucose, which is the primary constituent of exopolysaccharides in *S. mutans* biofilms (Bowen & Koo, 2011).

The lectins MNA-G, AAL, and ASA visualized the largest biovolumes and showed the brightest fluorescence intensities in the present study, which is in line with the results of Tawakoli et al. (2017). MNA-G specifically binds galactose, with only minor affinity to glucose and mannose (Rougé et al., 2003). Galactose is present in human saliva (Mandel et al., 1964) and is readily metabolized by organisms in dental biofilms, but it has only rarely been identified as a matrix component in biofilms of oral organisms. It is an important constituent of the exopolysaccharides produced by different highly pathogenic organisms (ESKAPE pathogens), such as *Pseudomonas aeruginosa* or *Klebsiella pneumoniae* (Bales et al., 2013; Ma et al., 2007), and it is also part of the matrix produced by *Candida albicans* (Baillie & Douglas, 2000), by different Lactobacilli (Cerning, 1990; Makino et al., 2006) and by the probiotic organism *Streptococcus thermophiles* (Xu et al., 2018). Interestingly, a recent study found that the water-soluble and insoluble exopolysaccharides produced by *S. mutans* contained 14% and 39% galactose, respectively, and that the matrix of a knockout mutant with attenuated adhesion and biofilm production was devoid of galactose (Lu et al., 2021). Across all 10 participants in the present study, MNA-G-bound biovolumes were very similar for biofilms grown in the presence

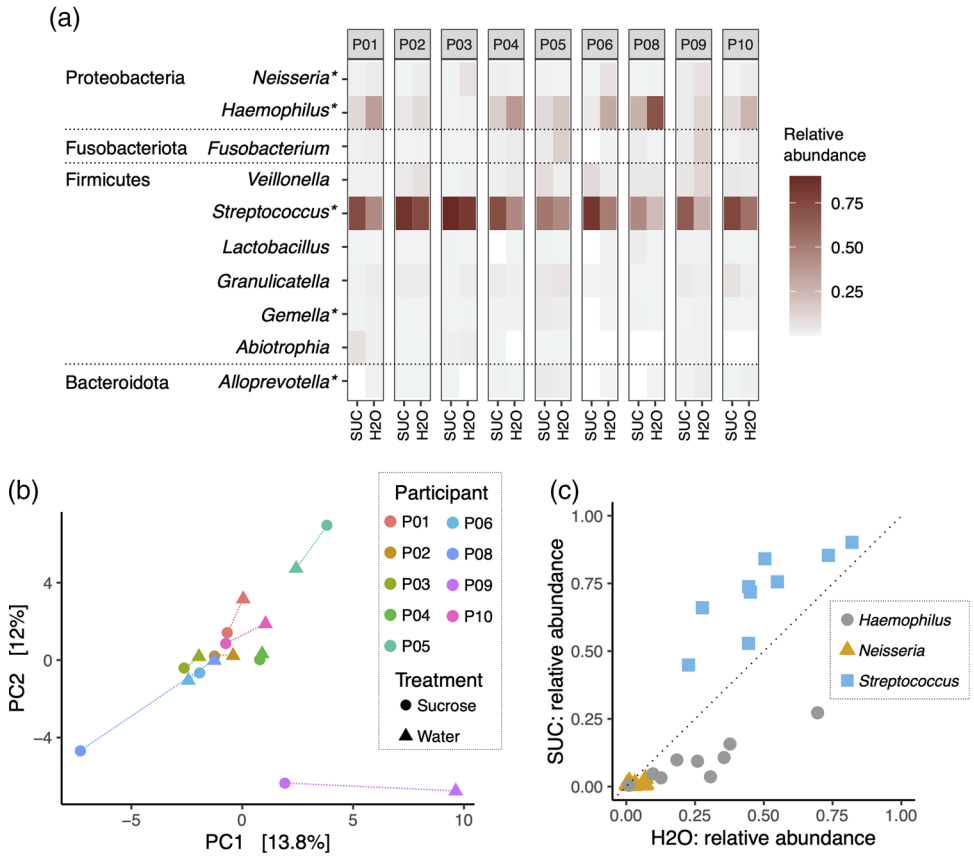

FIGURE 4 Bacterial community composition of the analyzed biofilms. (a) Heat map showing the relative abundance of the 10 most abundant genera across nine participants in biofilms grown in the presence (SUC) or absence (H2O) of sucrose (sequence data of participant 7 did not meet our quality criteria and were removed). Asterisks (*) indicate significant differences in the relative abundance of specific genera between SUC and H2O biofilms. For a list of all genera, see Table S3. (b) Principal component analysis (PCA) of clr-transformed read counts. Biofilm samples from the same participant generally group together, indicating that interindividual differences in community composition were larger than the effect of sucrose treatment. (c) Relative abundances of the three most abundant genera in SUC and H2O biofilms from the same participants. Exposure to sucrose significantly increased the relative abundance of *Streptococcus* spp. and decreased the abundance of *Haemophilus* spp. and *Neisseria* spp.

and absence of sucrose, which suggests that the microbial production of galactose-containing carbohydrates is not related to sucrose metabolism.

In contrast to MNA-G, biovolumes visualized by AAL and, especially, ASA were somewhat increased in biofilms exposed to sucrose during growth. AAL specifically binds fucose (Yamashita et al., 1985), whose role in dental biofilms remains largely unexplored. Fucose is present in salivary mucins that can be digested by complex microbial communities (Wickström & Svensäter, 2008), and its presence in dental biofilms has recently been associated with early childhood caries using a metabolomics approach (Heimisdottir et al., 2021). The lectin ASA has a high affinity to mannose (Dam et al., 1998), which is also a prominent component of the exopolysaccharide matrix of ESKAPE pathogens (Bales et al., 2013; Franklin et al., 2011). Intriguingly, several studies have identified mannose as the dominating component of the exopolysaccharide matrix of different oral organisms, such as *Prevotella intermedia*, *Prevotella nigrescens*, *Actinomyces oris*, and *Capnocytophaga ochracea* (Bolton & Dyer, 1983; Yamanaka et al., 2009; Yamane et al., 2005; Yamane et al., 2013). Recent work also identified mannose as part of the water-soluble and insoluble polysaccharides in *S. mutans* biofilms (Lu et al., 2021; Yang et al., 2019).

Taken together, these data clearly show that the role of glycoconjugates and exopolysaccharides other than glucans in dental biofilms merits further investigation. In the present study, we correlated the biovolumes of glycoconjugates/polysaccharides stained by MNA-G, AAL, or ASA with the abundance of bacterial genera in biofilms collected from the same participants. Biofilms exposed to sucrose during growth displayed not only increased AAL- and ASA-stained matrix biovolumes but also significantly higher relative abundances of *Streptococcus* spp. and lower abundances of *Haemophilus* spp. and *Neisseria* spp. However, the lectin-stained biovolumes varied considerably, not only between different participants but also between individual biofilms. As the biofilms were sacrificed during FLBA, sequencing had to be performed on different biofilm samples from the same participants. Using those biofilms, no significant correlation was observed between the abundance of specific bacterial genera and the biovolumes visualized by AAL, ASA, or MNA-G. Future work may strive to perform a combined analysis of carbohydrate components and the microbial

composition within the same biofilms, to identify correlations between the abundance of specific organisms and the carbohydrate matrix.

In conclusion, the present study demonstrated a high diversity of different matrix glycoconjugates/polysaccharides in in situ-grown dental biofilms. The lectins AAL, MNA-G, and ASA, with specific affinities for fucose, galactose, and mannose, respectively, visualized large biovolumes in dental biofilms grown in the absence and presence of sucrose. Lectin binding showed considerable variation between study participants and also between replicate biofilms from the same participant. The exact relationship between carbohydrate structures in the biofilm matrix and their microbial producers in complex dental biofilms remains to be elucidated.

ACKNOWLEDGMENTS

This study was supported by the Danish Dental Association (FORSKU). The authors would like to thank Lene Grønkjær and Anette Aakjær Thomsen for excellent technical support.

CONFLICT OF INTEREST

The authors declare no conflict of interest.

DATA AVAILABILITY STATEMENT

The data that support the findings of this study are available from the corresponding author upon reasonable request.

REFERENCES

Baillie, G. S., & Douglas, L. J. (2000). Matrix polymers of *Candida* biofilms and their possible role in biofilm resistance to antifungal agents. *The Journal of Antimicrobial Chemotherapy*, *46*(3), 397–403. https://doi.org/10.1093/jac/46.3.397

Bales, P. M., Renke, E. M., May, S. L., Shen, Y., & Nelson, D. C. (2013). Purification and characterization of biofilm-associated EPS exopolysaccharides from ESKAPE organisms and other pathogens. *PLoS ONE*, *8*(6), e67950. https://doi.org/10.1371/journal.pone.0067950

Banas, J. A., & Vickerman, M. M. (2003). Glucan-binding proteins of the oral streptococci. *Critical Reviews in Oral Biology and Medicine*, *14*(2), 89–99. https://doi.org/10.1177/154411130301400203

Bolton, R. W., & Dyer, J. K. (1983). Suppression of murine lymphocyte mitogen responses by exopolysaccharide from *Capnocytophaga ochracea*. *Infection and Immunity*, *39*(1), 476–479. https://doi.org/10.1128/iai.39.1.476-479.1983

Bowen, W. H., & Koo, H. (2011). Biology of Streptococcus mutans-derived glucosyltransferases: Role in extracellular matrix formation of cariogenic biofilms. *Caries Research*, *45*(1), 69–86. https://doi.org/10.1159/000324598

Bowen, W. H., Burne, R. A., Wu, H., & Koo, H. (2018). Oral biofilms: Pathogens, matrix, and polymicrobial interactions in microenvironments. *Trends in Microbiology*, *26*(3), 229–242. https://doi.org/10.1016/j.tim.2017.09.008

Callahan, B. J., McMurdie, P. J., Rosen, M. J., Han, A. W., Johnson, A. J. A., & Holmes, S. P. (2016). Dada2: High-resolution sample inference from Illumina amplicon data. *Nature Methods*, *13*(7), 581–583. https://doi.org/10.1038/nmeth.3869

Cerning, J. (1990). Exocellular polysaccharides produced by lactic acid bacteria. *FEMS Microbiology Reviews*, *87*(1-2), 113–130. https://doi.org/10.1111/j.1574-6968.1990.tb04883.x

Cugini, C., Shanmugam, M., Landge, N., & Ramasubbu, N. (2019). The role of exopolysaccharides in oral biofilms. *Journal of Dental Research*, *98*(7), 739–745. https://doi.org/10.1177/0022034519845001

Daims, H., Lücker, S., & Wagner, M. (2006). Daime, a novel image analysis program for microbial ecology and biofilm research. *Environmental Microbiology*, *8*(2), 200–213. https://doi.org/10.1111/j.1462-2920.2005.00880.x

Dam, T. K., Bachhawat, K., Rani, P. G., & Surolia, A. (1998). Garlic (*Allium sativum*) lectins bind to high mannose oligosaccharide chains. *The Journal of Biological Chemistry*, *273*(10), 5528–5535. https://doi.org/10.1074/jbc.273.10.5528

Davis, N. M., Proctor, D. M., Holmes, S. P., Relman, D. A., & Callahan, B. J. (2018). Simple statistical identification and removal of contaminant sequences in marker-gene and metagenomics data. *Microbiome*, *6*(1), 226. https://doi.org/10.1186/s40168-018-0605-2

Franklin, M. J., Nivens, D. E., Weadge, J. T., & Howell, P. L. (2011). Biosynthesis of the pseudomonas aeruginosa extracellular polysaccharides, alginate, Pel, and Psl. *Frontiers in Microbiology*, *2*, 167. https://doi.org/10.3389/fmicb.2011.00167

Gonçalves, L. M., Del Bel Cury, A. A., Vasconcellos, A. A. d., Cury, J. A., & da Silva, W. J. (2015). Confocal analysis of the exopolysaccharide matrix of *Candida albicans* biofilms. *Journal of Investigative and Clinical Dentistry*, *6*(3), 179–185. https://doi.org/10.1111/jicd.12093

Gundersen, H. J., & Jensen, E. B. (1987). The efficiency of systematic sampling in stereology and its prediction. *Journal of Microscopy*, *147*(Pt. 3), 229–263. https://doi.org/10.1111/j.1365-2818.1987.tb02837.x

Hannig, C., Gaeding, A., Basche, S., Richter, G., Helbig, R., & Hannig, M. (2013). Effect of conventional mouthrinses on initial bioadhesion to enamel and dentin in situ. *Caries Research*, *47*(2), 150–161. https://doi.org/10.1159/000345083

Heimisdottir, L. H., Lin, B. M., Cho, H., Orlenko, A., Ribeiro, A. A., Simon-Soro, A., Roach, J., Shungin, D., Ginnis, J., Simancas-Pallares, M. A., Spangler, H. D., Zandoná, A. G. F., Wright, J. T., Ramamoorthy, P., Moore, J. H., Koo, H., Wu, D., & Divaris, K. (2021). Metabolomics insights in early childhood caries. *Journal of Dental Research*, *100*(6), 615–622. https://doi.org/10.1177/0022034520982963

Herlemann, D. P., Labrenz, M., Jürgens, K., Bertilsson, S., Waniek, J. J., & Andersson, A. F. (2011). Transitions in bacterial communities along the 2000 km salinity gradient of the Baltic Sea. *The ISME Journal*, *5*(10), 1571–1579. https://doi.org/10.1038/ismej.2011.41

Hertel, S., Pötschke, S., Basche, S., Delius, J., Hoth-Hannig, W., Hannig, M., & Hannig, C. (2017). Effect of tannic acid on the protective properties of the in situ formed pellicle. *Caries Research*, *51*(1), 34–45. https://doi.org/10.1159/000451036

Hertel, S., Wolf, A., Basche, S., Viergutz, G., Rupf, S., Hannig, M., & Hannig, C. (2017). Initial microbial colonization of enamel in children with different levels of caries activity: An in situ study. *American Journal of Dentistry*, *30*(3), 171–176.

Jakubovics, N. S., Goodman, S. D., Mashburn-Warren, L., Stafford, G. P., & Cieplik, F. (2021). The dental plaque biofilm matrix. *Periodontology 2000*, *86*(1), 32–56. https://doi.org/10.1111/prd.12361

Karygianni, L., Ren, Z., Koo, H., & Thurnheer, T. (2020). Biofilm matrixome: Extracellular components in structured microbial communities. *Trends in Microbiology*, *28*(8), 668–681. https://doi.org/10.1016/j.tim.2020.03.016

Lahti, L., Shetty, S., & Salojarvi, J. (2017). *microbiome*. R package.

Lester, K., & Simmonds, R. S. (2012). Zoocin A and lauricidin in combination reduce *Streptococcus mutans* growth in a multispecies biofilm. *Caries Research*, *46*(3), 185–193. https://doi.org/10.1159/000337307

Lu, Y., Zhang, H., Li, M., Mao, M., Song, J., Deng, Y., Lei, L., Yang, Y., & Hu, T. (2021). The rnc gene regulates the microstructure of exopolysaccharide in the biofilm of *Streptococcus mutans* through the β-monosaccharides. *Caries Research*, *55*(5), 534–545. https://doi.org/10.1159/000518462

Ma, L., Lu, H., Sprinkle, A., Parsek, M. R., & Wozniak, D. J. (2007). Pseudomonas aeruginosa Psl is a galactose- and mannose-rich exopolysaccharide. *Journal of Bacteriology*, *189*(22), 8353–8356. https://doi.org/10.1128/JB.00620-07

Makino, S., Ikegami, S., Kano, H., Sashihara, T., Sugano, H., Horiuchi, H., Saito, T., & Oda, M. (2006). Immunomodulatory effects of polysaccharides produced by *Lactobacillus delbrueckii* ssp. *bulgaricus* OLL1073R-1. *Journal of Dairy Science*, *89*(8), 2873–2881. https://doi.org/10.3168/jds.S0022-0302(06)72560-7

Mandel, I. D., Thompson, R., & Ellison, S. A. (1964). The carbohydrate components of human submaxillary saliva. *Archives of Oral Biology*, *9*(6), 601–609. https://doi.org/10.1016/0003-9969(64)90074-3

Martin, M. (2011). Cutadapt removes adapter sequences from high-throughput sequencing reads. *EMBnet.Journal*, *17*(1), 10–12. https://doi.org/10.14806/ej.17.1.200

McMurdie, P. J., & Holmes, S. (2013). Phyloseq: An R package for reproducible interactive analysis and graphics of microbiome census data. *PLoS ONE*, *8*(4), e61217. https://doi.org/10.1371/journal.pone.0061217

Neu, T. R., & Lawrence, J. R. (1999). Lectin-binding analysis in biofilm systems. *Methods in Enzymology*, *310*, 145–152. https://doi.org/10.1016/S0076-6879(99)10012-0

Nobbs, A. H., Lamont, R. J., & Jenkinson, H. F. (2009). Streptococcus adherence and colonization. *Microbiology and Molecular Biology Reviews: MMBR*, *73*(3), 407–450. https://doi.org/10.1128/MMBR.00014-09

Oksanen, J., Blanchet, F. G., Kindt, R., Legendre, P., Minchin, P. R., O'Hara, R. B., Simpson, G. L., Solymos, P., Stevens, M. H. H., & Wagner, H. (2019). Vegan: *Community* ecology package. R Package.

Quast, C., Pruesse, E., Yilmaz, P., Gerken, J., Schweer, T., Yarza, P., Peplies, J., & Glöckner, F. O. (2013). The SILVA ribosomal RNA gene database project: Improved data processing and web-based tools. *Nucleic Acids Research*, *41*(Database issue), D590–D596. https://doi.org/10.1093/nar/gks1219

R Core Team. (2021). *R: Version 4.1.1*. R Foundation for Statistical Computing.

Rougé, P., Peumans, W. J., Barre, A., & van Damme, E. J. (2003). A structural basis for the difference in specificity between the two jacalin-related lectins from mulberry (*Morus nigra*) bark. *Biochemical and Biophysical Research Communications*, *304*(1), 91–97. https://doi.org/10.1016/S0006-291X(03)00538-2

Tawakoli, P. N., Neu, T. R., Busck, M. M., Kuhlicke, U., Schramm, A., Attin, T., Wiedemeier, D. B., & Schlafer, S. (2017). Visualizing the dental biofilm matrix by means of fluorescence lectin-binding analysis. *Journal of Oral Microbiology*, *9*(1), 1345581. https://doi.org/10.1080/20002297.2017.1345581

Whittaker, C. J., Klier, C. M., & Kolenbrander, P. E. (1996). Mechanisms of adhesion by oral bacteria. *Annual Review of Microbiology*, *50*, 513–552. https://doi.org/10.1146/annurev.micro.50.1.513

Wickham, H. (2016). *Ggplot2: Elegant graphics for data analysis* (2nd ed.). Springer International Publishing.

Wickström, C., & Svensäter, G. (2008). Salivary gel-forming mucin MUC5B—A nutrient for dental plaque bacteria. *Oral Microbiology and Immunology*, *23*(3), 177–182. https://doi.org/10.1111/j.1399-302X.2007.00407.x

Xu, Z., Guo, Q., Zhang, H., Wu, Y., Hang, X., & Ai, L. (2018). Exopolysaccharide produced by Streptococcus thermophiles S-3: Molecular, partial structural and rheological properties. *Carbohydrate Polymers*, *194*, 132–138. https://doi.org/10.1016/j.carbpol.2018.04.014

Yamanaka, T., Furukawa, T., Matsumoto-Mashimo, C., Yamane, K., Sugimori, C., Nambu, T., Mori, N., Nishikawa, H., Walker, C. B., Leung, K.-P., & Fukushima, H. (2009). Gene expression profile and pathogenicity of biofilm-forming Prevotella intermedia strain 17. *BMC Microbiology*, *9*, 11. https://doi.org/10.1186/1471-2180-9-11

Yamane, K., Nambu, T., Yamanaka, T., Ishihara, K., Tatami, T., Mashimo, C., Walker, C. B., Leung, K.-P., & Fukushima, H. (2013). Pathogenicity of exopolysaccharide-producing *Actinomyces oris* isolated from an apical abscess lesion. *International Endodontic Journal*, *46*(2), 145–154. https://doi.org/10.1111/j.1365-2591.2012.02099.x

Yamane, K., Yamanaka, T., Yamamoto, N., Furukawa, T., Fukushima, H., Walker, C. B., & Leung, K.-P. (2005). A novel exopolysaccharide from a clinical isolate of *Prevotella nigrescens*: Purification, chemical characterization and possible role in modifying human leukocyte phagocytosis. *Oral Microbiology and Immunology*, *20*(1), 1–9. https://doi.org/10.1111/j.1399-302X.2004.00178.x

Yamashita, K., Kochibe, N., Ohkura, T., Ueda, I., & Kobata, A. (1985). Fractionation of L-fucose-containing oligosaccharides on immobilized *Aleuria aurantia* lectin. *The Journal of Biological Chemistry*, *260*(8), 4688–4693.

Yang, Y., Mao, M., Lei, L., Li, M., Yin, J., Ma, X., Tao, X., Yang, Y., & Hu, T. (2019). Regulation of water-soluble glucan synthesis by the *Streptococcus mutans* dexA gene effects biofilm aggregation and cariogenic pathogenicity. *Molecular Oral Microbiology*, *34*(2), 51–63. https://doi.org/10.1111/omi.12253

Falsetta, M. L., Klein, M. I., Colonne, P. M., Scott-Anne, K., Gregoire, S., Pai, C. H., Gonzalez-Begne, M., Watson, G., Krysan, D. J., Bowen, W. H., & Koo, H. (2014). Symbiotic relationship between *Streptococcus mutans* and *Candida albicans* synergizes virulence of plaque biofilms in vivo. *Infection and Immunity*, *82*(5), 1968–81. https://doi.org/10.1128/IAI.00087-1

SUPPORTING INFORMATION

Additional supporting information can be found online in the Supporting Information section at the end of this article.

How to cite this article: Dige, I., Paqué, P. N., Del Rey, Y. C., Lund, M. B., Schramm, A., & Schlafer, S. (2022). Fluorescence lectin binding analysis of carbohydrate components in dental biofilms grown in situ in the presence or absence of sucrose. *Molecular Oral Microbiology*, *37*, 196–205. https://doi.org/10.1111/omi.12384